

Isospin Separation of Three-Nucleon Form Factors

A. Amroun,^{(1),(a)} V. Breton,^{(1),(b)} J.-M. Cavedon,⁽¹⁾ B. Frois,⁽¹⁾ D. Goutte,⁽¹⁾ J. Martino,⁽¹⁾
 X.-H. Phan,⁽¹⁾ S. K. Platchkov,⁽¹⁾ I. Sick,⁽²⁾ and S. Williamson⁽³⁾

⁽¹⁾*DAPNIA, Service de Physique Nucléaire, Centre d'Études Nucléaires de Saclay, F-91191 Gif-sur-Yvette, France*

⁽²⁾*Institut für Physik, Universität Basel, CH-4056 Basel, Switzerland*

⁽³⁾*Nuclear Physics Laboratory and Department of Physics, University of Illinois, Champaign, Illinois 61820*

(Received 26 March 1992)

We have performed high-precision measurements of ^3He charge and magnetic form factors up to $Q^2=1$ (GeV/c)². These measurements combined with previous data on ^3He and ^3H allow us to separate the three-nucleon isospin charge and magnetic form factors up to $Q^2=1$ (GeV/c)². A large discrepancy between experiment and theory occurs for the $T=1$ charge form factor.

PACS numbers: 25.30.Bf, 25.10.+s, 27.10.+h

Two- and three-nucleon form factors are a subject of particular interest since they can be calculated from the nucleon-nucleon interaction in a reliable way. Several groups have now achieved high-accuracy numerical solutions of the three-nucleon problem including two- and three-nucleon forces [1]. At large momentum transfer the form factors corresponding to a purely nucleonic description differ substantially from experiment. Non-nucleonic degrees of freedom, such as meson-exchange currents, have been identified as the main sources for the observed discrepancies. For recent reviews see Refs. [2,3].

The trinucleon charge and magnetic form factors are linear combinations of isoscalar and isovector components. Isoscalar and isovector observables have different sensitivities to nucleonic and mesonic contributions. A separation of these components thus gives additional insight into the electromagnetic current operator and the structure of the three-nucleon system. This separation is of particular interest in the region of the impulse approximation diffraction minima, where the purely nucleonic contributions become small. The ($T=0$)-($T=1$) separation also permits a direct comparison to the other fully calculable system, the deuteron. Elastic scattering from the deuteron, a pure $T=0$ system, involves the same electromagnetic operators as those occurring for the $A=3$ isoscalar form factors. Deuteron electrodisintegration at threshold involves the same electromagnetic operators occurring in the $A=3$ isovector magnetic form factor.

Although a large amount of data exist on elastic electron scattering from ^3H and ^3He [4-13], the data on the charge and magnetic form factors for ^3He in the region of the diffraction minimum and second maximum were of limited accuracy [7,10]. Thus, in order to achieve a reliable isospin separation of the $A=3$ form factors we have performed a high-precision measurement of the elastic electron scattering cross section from ^3He up to $Q^2=1$ (GeV/c)².

This experiment was performed at Saclay with the 700-MeV electron linear accelerator and the HE1 experimental setup. The ^3He target was a gas cell, operating at

a temperature of 20 K and a pressure of 13 bars. The target thickness seen by the detection system at 90° was $425 \text{ mg}/\text{cm}^2$. The target and the liquid-hydrogen heat exchanger were placed in a vertical loop, with a fan enforcing rapid circulation of the ^3He cold gas. The diameter of the target (80 mm) was chosen such that the windows (7- μm steel) were outside the spectrometer acceptance. Background was negligible. For the extreme angles (25° , 155°) where the steel window would overlap with the tail of the acceptance function, a collimator close to the target eliminated all window contributions. The small effects of heating of the target at high beam intensity (up to 20 μA) were determined by measuring the rate of scattered electrons as a function of beam current and were found to be $0.4\%/\mu\text{A}$. A Faraday cup and two ferrite toroid monitors measured the beam current. The scattered electrons were analyzed using the SP900 high-energy-resolution (10^{-4}) magnetic spectrometer. The solid angle for a point target at the spectrometer pivot was precisely known from the geometry and spectrometer slit area. For an extended target, the dependence of the solid angle on the position along the beam direction was measured by displacing a thin solid target along the beam. The momentum-analyzed electrons were detected using the focal plane detector consisting of four planes of multiwire proportional chambers, two planes of scintillator detectors, and a gas Čerenkov counter. The inefficiencies of the various elements were measured by exploiting the redundancy of the detector setup.

Data were taken over a range of eight energies (315-640 MeV) and several angles (30° - 155°). Effects of kinematical broadening and finite target thickness were minimized by reconstructing the scattering vertex along the beam. The energy resolution was 1.5 MeV, sufficient to isolate the elastic peak. Standard radiative corrections were applied. The resulting data set of 45 cross sections covers a range of $Q^2=0.04$ -1 (GeV/c)². The systematic uncertainty of the cross sections, 2%, stems from uncertainties in the measurement of beam current, target thickness, spectrometer solid angle, and detector efficiency. The experimental cross sections have

been corrected for the small effects of Coulomb distortion, using phase-shift analysis for both electric and magnetic scattering. The standard radiative corrections were applied. Our new data significantly improve the accuracy of the ^3He charge from factor in the region of the first diffraction minimum and second diffraction maximum. This improvement reduces the uncertainty of the charge contribution in the measurement of the cross sections at backward angles. Consequently, when using the cross sections of Ref. [10], one also achieves a better determination of the magnetic form factor. A more detailed description of the experiment and data reduction will be given in a forthcoming publication. (A table of the new data for ^3He is available on request from the authors.)

For the determination of the isospin-separated form factors we have used, in addition to our new data, the complete world set of form factors measured for ^3H and ^3He . For ^3H we employ the data of Refs. [4,5,13]. For ^3He we include the data of Refs. [5-13]. For ^3H (^3He) we thus have a total of 184 (295) data points. In order to extract ^3H , ^3He charge, magnetic, and $T=0,1$ form factors the usual procedure, based on the Rosenbluth separation, requires data at exactly the same q^2 . This method is highly inefficient because it requires many retunings of the accelerator to get the same momentum transfer at varying scattering angles. Furthermore, one cannot use the results of experiments performed in different kinematic conditions. We have used the procedure developed previously to analyze our ^3H data [4]. The four standard form factors F_c^{H} , F_m^{H} , F_c^{He} , F_m^{He} (the Q^2 dependence has been omitted for clarity) were parametrized using the sum-of-Gaussians expansion of Ref. [14]. Each of the four form factors has twelve free parameters. The charge and magnetic form factors for both ^3H and ^3He were determined by simultaneously fitting the available set of cross sections at all energies and angles.

The statistical errors of the data points are used during the fitting process and yield the random uncertainty of the form factors via the error matrix. The effect of the systematic uncertainties was calculated by changing each individual data set by its quoted error, refitting the data, and summing quadratically all the resulting changes in the extracted values of the form factors.

The isospin-separated form factors F_c^0 , F_c^1 , F_m^0 , F_m^1 have been derived from the standard form factors F_c^{H} , F_m^{H} , F_c^{He} , F_m^{He} using the following relations:

$$2F_c^0 = F_c^{\text{H}} + 2F_c^{\text{He}}, \quad 2F_c^1 = -F_c^{\text{H}} + 2F_c^{\text{He}},$$

$$2F_m^0 = \mu_{\text{H}}F_m^{\text{H}} + \mu_{\text{He}}F_m^{\text{He}}, \quad 2F_m^1 = -\mu_{\text{H}}F_m^{\text{H}} + \mu_{\text{He}}F_m^{\text{He}},$$

where μ_{H} , μ_{He} are the $A=3$ magnetic moments, and where the F_c^{H} , F_c^{He} , F_m^{H} , F_m^{He} are normalized to $F(0)=1$.

The resulting values for the $A=3$ form factors are shown in Figs. 1 and 2. The numerical values for the parameters and error bands, either in terms of H (He) or $T=0$ (1) form factors, will be given in a more detailed publication. The error bands given in Figs. 1 and 2 repre-

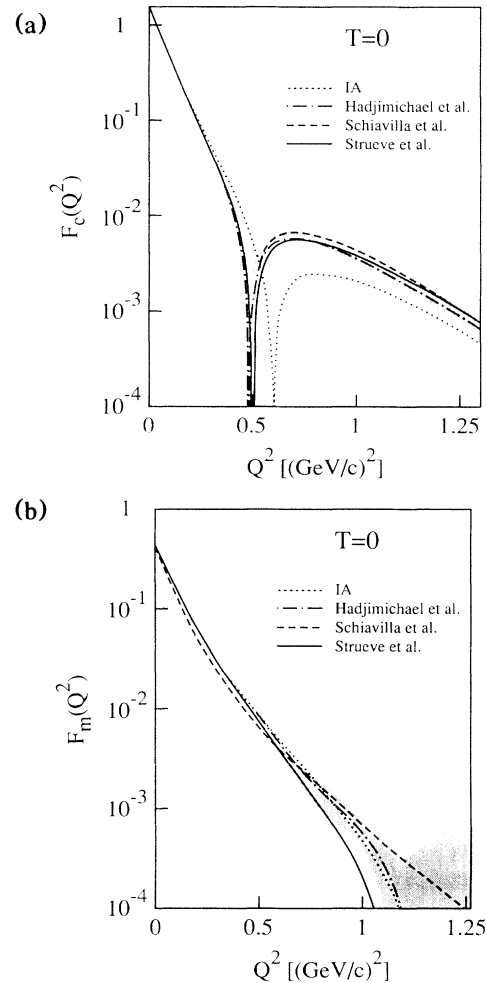


FIG. 1. Three-nucleon (a) charge and (b) magnetic isoscalar form factors. The error band shows the experimental values including statistical and systematic uncertainties. The curves represent the full calculations of Struete *et al.* [15], Hadjimichael, Goulard, and Bornais [16], and Schiavilla, Pandharipande, and Riska [17]. The nucleon contribution (impulse approximation) is depicted by the curve denoted IA [15].

sent the more reliable and complete information available on the $A=3$ form factors. These errors are derived from the world set of data; they include the contribution of both statistical and systematic uncertainties. The parametrization of the form factors is characterized by the introduction of a physical cutoff, the maximum radius $R=6$ fm, within which all charge and magnetism are distributed. This cutoff corresponds to a minimum wavelength of oscillations of $F(Q^2)$ "smoothed" over an interval $\Delta Q^2 \sim 0.0025$ $(\text{GeV}/c)^2$.

Figures 1 and 2 show that the $A=3$ form factors are now determined with good precision up to $Q^2=1$ $(\text{GeV}/c)^2$; previously, separate values for $T=0$ and 1 were available only at momentum transfers below the diffraction minima [$Q^2 \leq 0.32$ $(\text{GeV}/c)^2$]. For all except F_m^0 , the position of the minimum and the amplitude of the

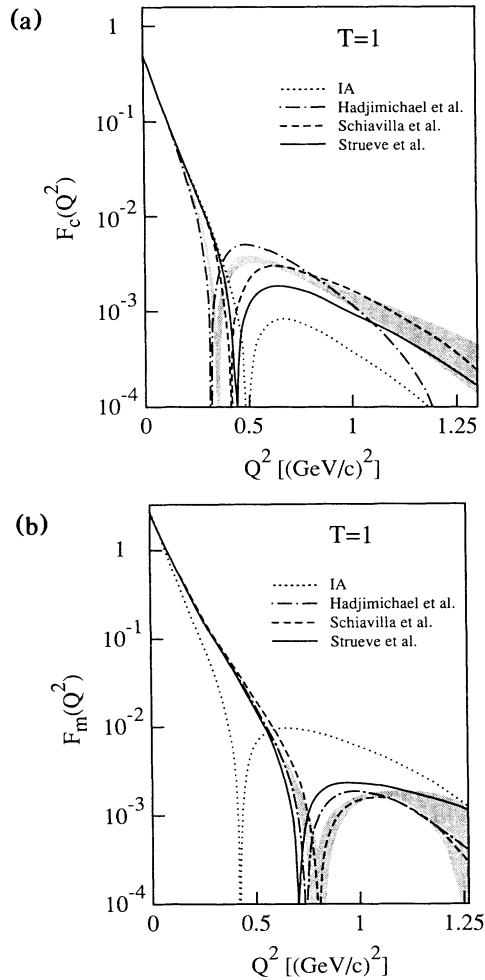


FIG. 2. Three-nucleon (a) charge and (b) magnetic form isovector factors. See caption of Fig. 1.

following diffraction maximum are well defined. The increase in the uncertainty at large Q^2 is mainly linked to the limitations in our knowledge of charge scattering from ^3H . In Figs. 1 and 2 we compare our data to the results of a number of modern calculations. The results of Strueve *et al.* [15] are obtained from a coupled-channel Faddeev calculation in momentum space. This approach is based on a consistent treatment of the nucleon-nucleon and nucleon-delta channels. The interactions used are derived from the Paris N - N potential, and give a good description of the inelastic channels involving pions. The contributions of π - and ρ -exchange currents as well as relativistic corrections are taken into account. We also show the purely nucleonic contribution (impulse approximation) [15], in order to gauge the effect of non-nucleonic degrees of freedom.

The calculation of Hadjimichael, Goulard, and Bornais [16] corresponds to a solution of the Faddeev equations for the Sprung-de Toureil N - N potential; the exchange currents involving pions and deltas are added. The re-

sults of Schiavilla, Pandharipande, and Riska [17] are based on a variational three-body wave function, calculated using the Argonne v_{14} interaction and the Urbana model for the three-body force. In this calculation the π -like and ρ -like exchange currents are derived directly from the N - N interaction in a consistent way. The results of the different calculations in terms of nucleons only are quite similar for both charge and magnetic form factors.

The comparison between experiment and the full theoretical calculations allows the following observations.

(i) The impulse approximation calculation needs and gets a large correction from meson-exchange currents for the $T=0$ charge form factor and it is remarkable how good the agreement is between the data and all three calculations. The contributions of three-nucleon forces predicted by these calculations are small. The fact that the meson-exchange currents do so well for the charge form factor is unexpected given the conceptual uncertainties in the $T=0$ meson-exchange currents for F_c . Meson-exchange currents are suppressed by a factor of $(v/c)^2$ relative to the impulse approximation contribution for charge form factors, and are of the same order as relativistic kinematic corrections to the one-body currents. Theory is not yet in a position to describe these meson-exchange currents with a clear hierarchy in a consistent framework as is the case for $T=1$ magnetic transitions. Thus meson-exchange current contributions are only estimated in a perturbative expansion of the electromagnetic operators as a function of (v/c) . For the $T=0$ magnetic form factor, the three models shown have qualitatively different behavior above $Q^2=0.8$ $(\text{GeV}/c)^2$. But, below this value, theory is in good agreement with experiment for both charge and magnetic $T=0$ form factors. Apart from the slight deviation of the calculation of Schiavilla, Pandharipande, and Riska [17] for the $T=0$ magnetic form factor at low q that is not understood, there are only small differences between the predictions of realistic nucleon-nucleon potentials. These results indicate that up to $Q^2=0.8$ $(\text{GeV}/c)^2$ the description of two-body currents in the three-nucleon system is constrained by data on the two-nucleon system and that three-nucleon wave functions are well described by modern calculations.

(ii) For the $T=1$ magnetic form factor we also observe reasonable agreement between experiment and theory. As expected from deuteron electrodisintegration data [3,18,19] there is a very large contribution of meson-exchange currents. This confirms the importance of the role of meson-exchange currents in isovector magnetic transitions. The meson-exchange-current contributions are larger for the calculation of Schiavilla, Pandharipande, and Riska [17], mainly due to the pionlike pseudoscalar component. This contribution is partly canceled through the use of the G_E^V form factor for the exchange-current operator; in the calculation of Strueve *et al.* [15] the F_1^V form factor is employed instead. This corresponds to corrections that are of higher relativistic order.

(iii) There are large differences between the calculated $T=1$ charge form factors. No calculation describes the data. Therefore it is likely that it is this specific isospin component that is the origin of the long-standing discrepancy observed between theory and experiment for the charge form factors of ${}^3\text{H}$ and ${}^3\text{He}$.

In conclusion, we have performed an accurate isospin separation of the form factors of the three-nucleon system up to $Q^2=1$ $(\text{GeV}/c)^2$. The data are in general well described by theory in terms of nucleons and mesons. Non-nucleonic degrees of freedom and relativistic corrections make a significant contribution, and are important in getting theory in agreement with experiment. Relativistic effects are only approximated and thus remain a source of theoretical uncertainty. A large discrepancy between experiment and theory occurs for the $T=1$ charge form factor. Contrary to all the other three-nucleon form factors, this observable cannot be isolated in the $A=2$ system. The understanding of this new experimental information on the three-nucleon system is a challenge. This will require a consistent description of the two- and three-nucleon systems.

Future measurements in the energy range of CEBAF ($E \leq 4$ GeV) will be of great interest to find the diffractive structure of the trinucleon form factors beyond $Q^2=1$ $(\text{GeV}/c)^2$. Diffraction minima are due to cancellations between various amplitudes, and their positions are very sensitive to theoretical hypotheses. The observation of new diffraction minima would be of great help in disentangling the nature of the different currents contributing to the trinucleon form factors.

We are very grateful to J. F. Mathiot, P. Sauer, and J. Tjon for illuminating discussions on this work. We would

also like to thank L. Maximon for his very helpful comments.

^(a)Present address: Université d'Alger, Alger, Algérie.

^(b)Present address: Université de Clermont-Ferrand, Clermont-Ferrand, France.

- [1] *The Three-Body Force in the Three-Nucleon System*, edited by B. L. Berman and B. F. Gibson, Lecture Notes in Physics Vol. 260 (Springer-Verlag, Berlin, 1986).
- [2] *Modern Topics in Electron Scattering*, edited by B. Frois and I. Sick (World Scientific, Singapore, 1991).
- [3] J-F. Mathiot, Phys. Rep. **173**, 63 (1989).
- [4] F-P. Juster *et al.*, Phys. Rev. Lett. **55**, 2261 (1985).
- [5] H. Collard *et al.*, Phys. Rev. **138**, B57 (1965).
- [6] M. Bernheim *et al.*, Nuovo Cimento **5**, 431 (1972).
- [7] J. S. McCarthy, I. Sick, and R. R. Whitney, Phys. Rev. C **15**, 1396 (1977), and references therein.
- [8] Z. M. Szalata *et al.*, Phys. Rev. C **15**, 1200 (1977).
- [9] R. G. Arnold *et al.*, Phys. Rev. Lett. **40**, 1429 (1978).
- [10] J. M. Cavedon, Phys. Rev. Lett. **49**, 986 (1982).
- [11] P. C. Dunn *et al.*, Phys. Rev. C **27**, 71 (1983).
- [12] C. R. Ottermann *et al.*, Nucl. Phys. **A435**, 688 (1985).
- [13] D. Beck *et al.*, Phys. Rev. Lett. **59**, 1537 (1987).
- [14] I. Sick, Nucl. Phys. **A218**, 509 (1974).
- [15] W. Struewe, Ch. Hajduk, P. U. Sauer, and W. Theis, Nucl. Phys. **A465**, 651 (1987).
- [16] E. Hadjimichael, B. Goulard, and R. Bornais, Phys. Rev. C **27**, 831 (1983).
- [17] R. Schiavilla, V. J. Pandharipande, and D. O. Riska, Phys. Rev. C **40**, 2294 (1989); **41**, 309 (1990).
- [18] K. S. Lee *et al.*, Phys. Rev. Lett. **67**, 2634 (1991).
- [19] R. Schiavilla and D. O. Riska, Phys. Rev. C **43**, 437 (1991).

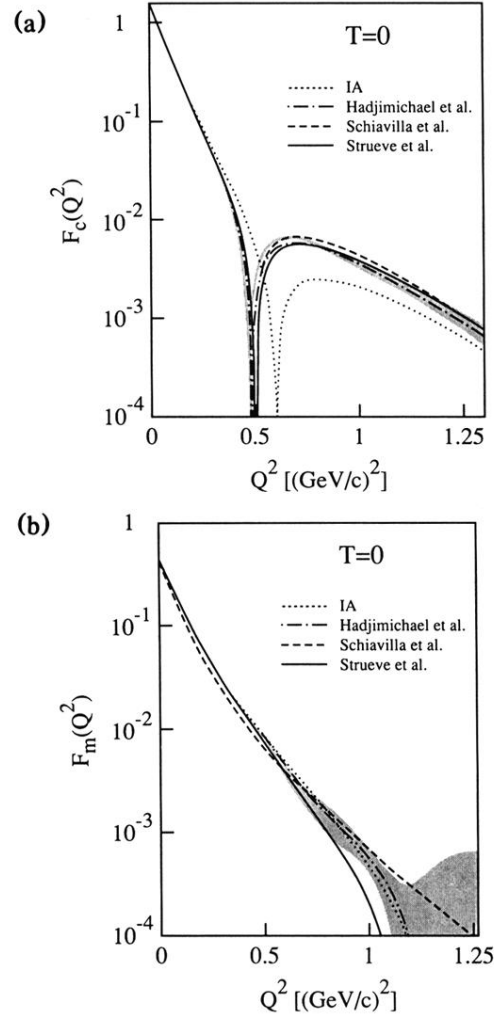


FIG. 1. Three-nucleon (a) charge and (b) magnetic isoscalar form factors. The error band shows the experimental values including statistical and systematic uncertainties. The curves represent the full calculations of Strueve *et al.* [15], Hadjimichael, Goulard, and Bornais [16], and Schiavilla, Pandharipande, and Riska [17]. The nucleon contribution (impulse approximation) is depicted by the curve denoted IA [15].

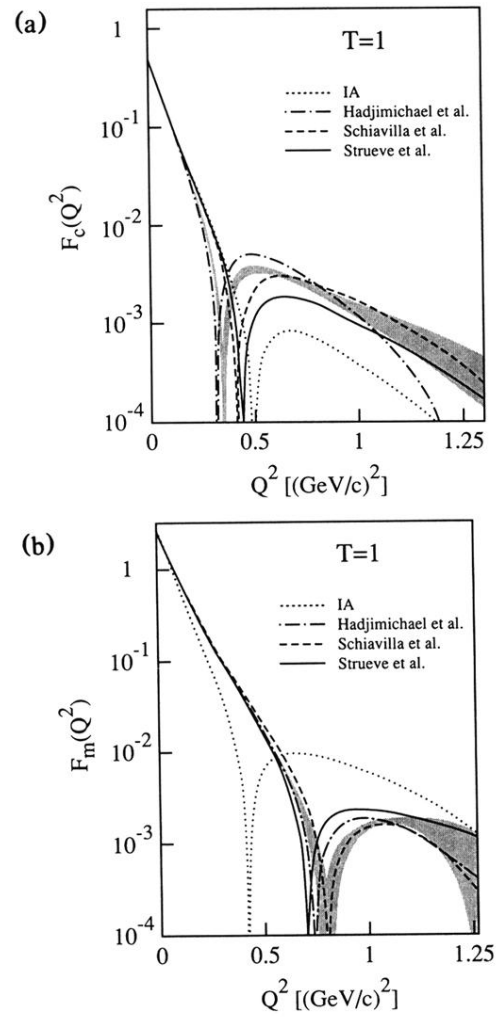


FIG. 2. Three-nucleon (a) charge and (b) magnetic form isovector factors. See caption of Fig. 1.